# DC-side Impedance for Handling Interoperability of Multi-vendor Multi-terminal HVDC Systems

Ashkan Nami*, Adil Abdalrahman, Ying-Jiang Häfner, Malaya Kumar Sahu,
and Khirod Kumar Nayak
Hitachi Energy - HVDC, Ludvika, Sweden
*Email: ashkan.nami1@hitachienergy.com

## Keywords

≪Interoperability≫, ≪DC stability≫, ≪HVDC≫, ≪DC impedance≫, ≪Impedance scanning≫

## Abstract

Using equivalent impedance to address possible interoperability issues is a well-established practice in electric rail systems and it is also a feasible approach for investigating DC-side control interactions, thereby avoiding or mitigating possible interoperability issues in multi-vendor multi-terminal high voltage direct current (HVDC) systems. This paper presents different aspects related to DC-side equivalent impedances which may be necessary to be considered in practice.

## Introduction

In addressing the challenges of shifting from a fossil fuel-based to renewable energy-based powers, the application of high voltage direct current (HVDC) transmissions is continuously increased. In particular, considering the intermittency and spatial disparity of renewable energy generation, interconnecting the renewable powers from a wide area on the DC side and developing multi-terminal DC (MTDC) networks have recently received an increasing interest [1]-[3] in order to achieve operational flexibility and power supply sustainability. In MTDC, there will be at least one power converter at each terminal or node. The dynamic behaviors and steady-state characters of power converters are highly dependent on control design. The converter control is the core intellectual property (IP) of power converter manufactures from all types of industries including HVDC. Due to black-box character of HVDC control, the interoperability issue draws attention to multi-vendor multi-terminal HVDC system developers as well as researchers. It should be mentioned that the interoperability issue related to power converters is not new and established practices as well as standards/guidelines are available since decades [4]. It has been shown in railway application that using equivalent impedance to characterize the active element such as power converter and to assess the stability is very effective. Therefore, using equivalent impedance for HVDC converter can be a good approach to address the interoperability issue related to multi-vendor MTDC systems.

Since the finding of DC oscillation in a MTDC with multi-vendors [5], a number of studies related to using impedance to assess DC network stability have been published in the literature. In [6]-[8], a stability analysis based on an analytical analysis of models of HVDC converters or entire MTDC systems is proposed in which detailed knowledge of the converter control systems is needed. However, analytical expression of the equivalent converter DC-side impedance is very complex. Modular multilevel converter (MMC) based HVDC stations may be far more complicated to be described by simple analytical forms due to physical limits in the main circuit equipment (voltage, current rating, temperature, etc.). Furthermore, the dynamics of each converter cell may be difficult to be represented in simple analytical forms [9]. Although the use of an average model could avoid the complexity, it may miss some significant dynamic properties. Moreover, significant details of the converter and its corresponding control are needed in those methods which is not suitable for multi-vendor applications [10].

Therefore, methods which allow protecting the IP of vendors (while giving more realistic representation) can facilitate impedance-based stability analysis in multi-vendor MTDC systems. For this purpose, methods based on the detailed impedance measurements utilizing a frequency sweep approach [11]-[14] can be used. Reference [15] presents an effective equivalent impedance calculation method for control stability assessment in HVDC grids with the main contribution of impedance combination of different elements. This leads to highly-accurate impedances of radial MTDC networks being achieved in a very short time. However, the considered MTDC is based on symmetrical monopole meaning each terminal has only one converter. References [16] and [17] introduce a PSCAD-compatible software toolbox that enables the accurate impedance measurement of MMC while in [17], a bipolar HVDC system with metallic return is considered. However, none of those references address (a) the details of considered impedance scanning setups, (b) HVDC relevant scanning frequency range, and (c) impact of AC network conditions on the scanned impedances.

The aim of this paper is to address the aforementioned issues and as a result, to share some relevant study experiences as a vendor with a lot of real project experiences. In the following section, the study experiences is presented which is split into five different subsections: 1) the scanning setup in both monopole and bipolar, 2) the scanning frequency range, 3) the impact of the AC network on the equivalent DC-side impedance, 4) the impact of load level of converter, and 5) the impact of DC system configuration. Finally, a summary of the studies is given.

## DC-side Impedance Scanning – Study Experiences

### DC-side Impedance Scanning Setup

To enable the active power flow over the HVDC link from one station to other station, one station is operated in DC voltage control ($U_{dc}$-control) mode while other station is operated in active power control (P-control) mode. There are other control modes as well such as islanding (frequency-voltage) control mode of operation where converter regulates neither DC voltage nor active power. Accordingly, a converter under test sees other station as a current source (when it is operated in $U_{dc}$-control mode) or a voltage source (when it is operated in power or islanding control mode) at its DC-side. Thus, depending on the control mode, the impedance scan circuit on DC-side varies. It is also worthwhile to investigate the impact of one pole converter on another pole converter in a bipolar system. Therefore, the test circuits are discussed for both monopole and bipolar systems.

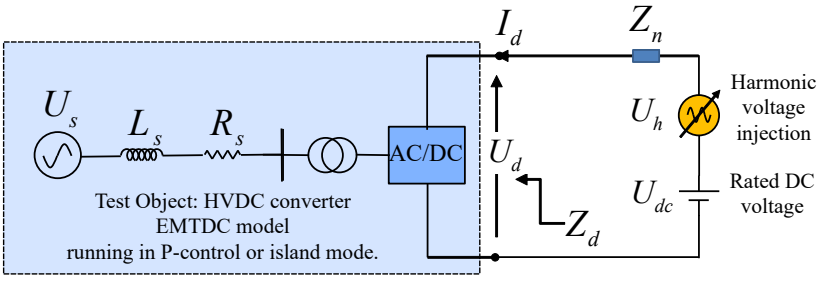


Fig. 1: Test circuit for measuring impedance seen from the DC-side of a converter operating in P-control or islanding control mode.

Fig. 1 shows the test circuit for scanning the DC-side impedance of a P-controlling or islanding control station in a monopole configuration. Note that a detailed switching model of converter provided by the manufacturer is used in the test circuits proposed throughout this paper. Moreover, any passive element connected in series and shunt to ground on the DC-side can be excluded from the test object leading to only active element being seen from the DC-port. Therefore, those passive elements can be considered as a part of DC network which are not shown in Fig. 1 for the sake of clarity. $U_{dc}$-controlling station can be represented by an equivalent DC voltage source behind a series impedance ($Z_n$) or by an ideal DC voltage source whose voltage is set equal to the rated DC voltage of HVDC link. As the objective

is to measure the impedance inserted by the converter which is an active element, a variable AC voltage source is also added in series with the DC voltage source in order to perform an impedance scanning at various frequencies. Therefore, the impedance scanning can be performed by driving sufficient harmonic currents to the test object and measuring the voltage drops across it. It is worth mentioning that the AC voltage source magnitude ($U_h$) needs to be kept below a certain level in order to ensure that any protection is not activated while injecting harmonic voltages. The frequency of the AC voltage source can be varied over a wide range of interest. Finally, the impedance seen from the DC-side ($Z_d$) is measured as given by (1).

$$Z_d = \frac{U_d}{I_d} \tag{1}$$

where $U_d$ is the voltage across the test object and $I_d$ is the current driven to the test object.

Fig. 2 shows DC-side impedance scanning results for a part of frequency range of interest from two different setups: the test circuit shown in Fig. 1 and a point-to-point HVDC system. From these results, it can be concluded that either setup can be used as there is very little difference between the results of the two setups in both real and imaginary parts of the DC-side impedance ($Z_{re}$ and $Z_{im}$, respectively).

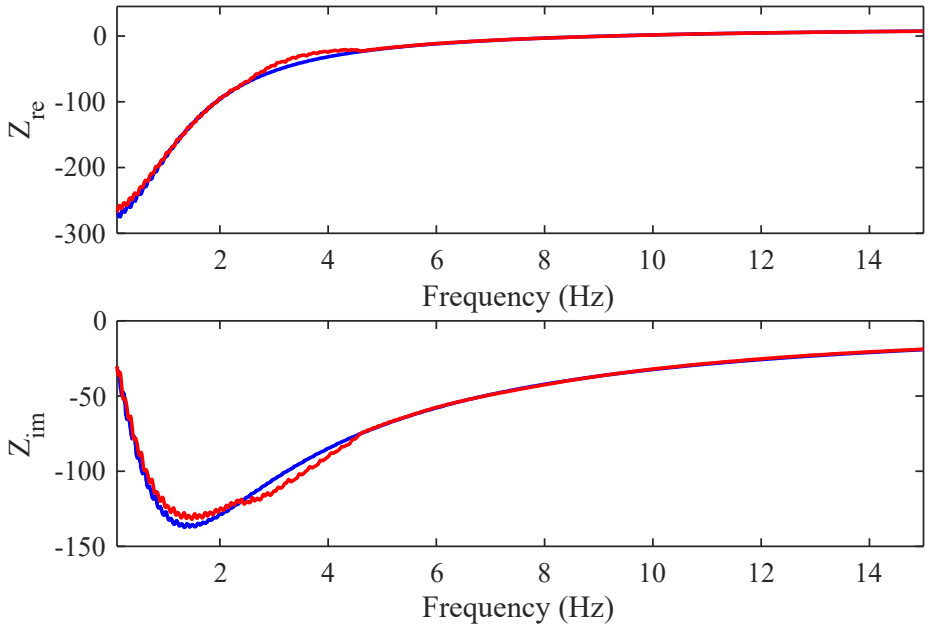


Fig. 2: DC-side impedance scanning results for P-controlling station from the proposed test circuit (blue color) and a point-to-point HVDC system (red color).

Moreover, Fig. 3 shows the test circuit for scanning the DC-side impedance of a bipolar converter station operated in P-control or islanding control mode. Note that the bipolar configuration has a neutral pole which can be a ground electrode via ground impedance, or a metallic return to other station or can be floating point (rigid-bipolar). To investigate the impact of one pole converter dynamics on the other pole converter dynamics, the DC-side impedance can be measured for individual pole converters while any neutral impedance connected to ground is kept as a part of outer circuit (see Fig. 3). The DC-side impedances of both positive and negative pole converters ($Z_{dp}$ and $Z_{dn}$, respectively) can be represented by following equations:

$$Z_{dp} = \frac{U_{dp}}{I_{dp}} \tag{2}$$

$$Z_{dn} = \frac{U_{dn}}{I_{dn}} \tag{3}$$

where $U_{dp}$ and $U_{dn}$ are the voltages across the positive and negative test objects, respectively. $I_{dp}$ and $I_{dn}$ are the currents driven to the positive and negative test objects, respectively.

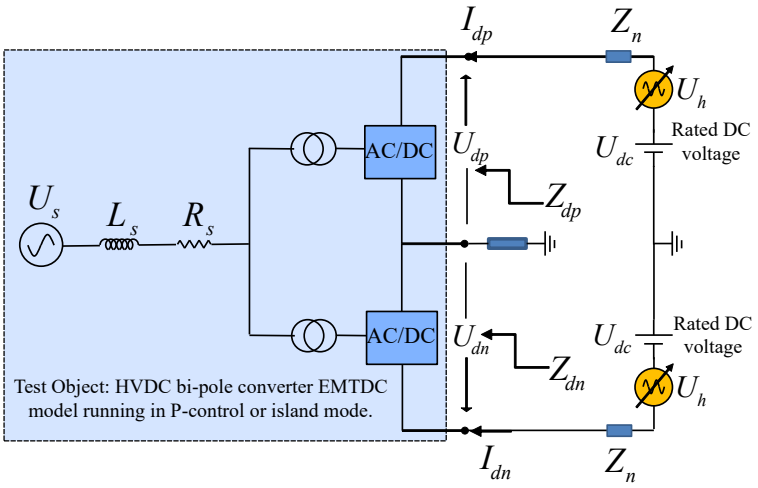


Fig. 3: Test circuit for measuring impedances seen from the DC-side in a bipolar configuration while operating in P-control or islanding control mode.

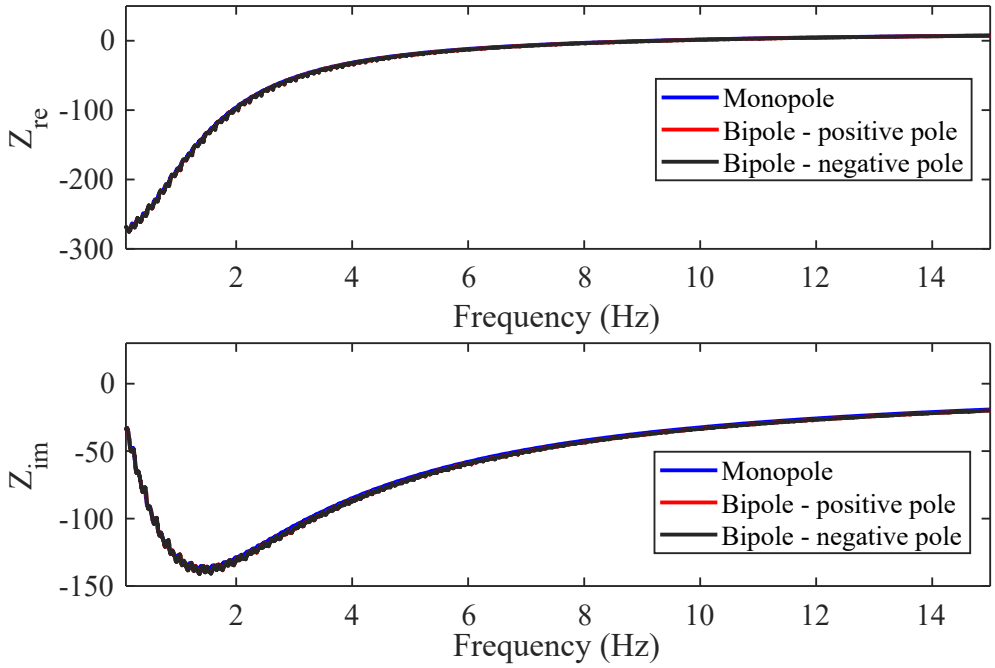


Fig. 4: DC-side impedance seen for monopole (blue color), for positive pole converter (red color) and for negative pole converter (black color) in bipolar with ground return configuration while operating in P-control mode.

It turns out that there is no cross-coupling impedance when both active and passive elements in bipolar system are symmetrical, and the impedances expressed in (1), (2) and (3) are almost equal under all scanned frequencies for the station with direct or indirect grounding. Fig. 4 shows a comparison of scanned DC-side impedances for a part of frequency range of interest from the test circuits depicted in Fig. 1 and Fig. 3. According to this comparison, the pole self-impedance in bipolar is similar to the

DC-side impedance in monopole. This means that it is possible to consider only the monopole system for stability analyzing which, in generic, could significantly simplify the stability analysis.

Finally, Fig. 5 shows the test circuit for measuring DC-side impedance of $U_{dc}$-controlling station in monopole configuration. Similarly, any passive element connected at DC pole can be kept as a part of DC network While P-controlling station can be represented by a DC current source behind a parallel admittance ($Y_n$) or an ideal DC current source whose current is set equal to the rated DC current. In order to scan the impedance seen from the converter DC terminal at different frequencies, an AC current source is connected in parallel with the DC current source (see Fig. 5). It is also worth mentioning that the AC current source magnitude ($I_h$) needs to be kept very low to ensure that any protection is not activated while injecting harmonic currents.

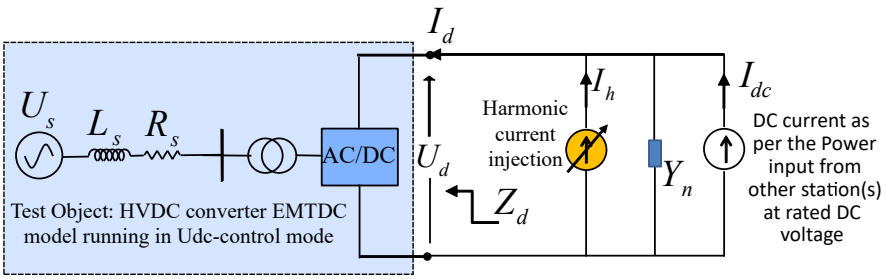


Fig. 5: Test circuit for measuring impedance seen from the DC-side of a $U_{dc}$-control station.

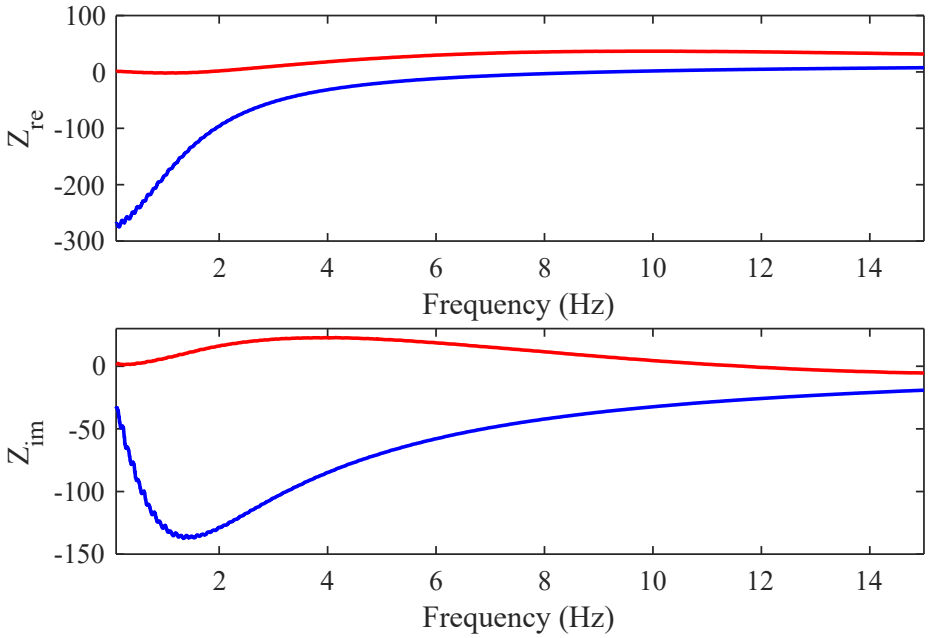


Fig. 6: Example of DC-side impedance of MMC in low frequency for both P-controlling station (blue color) and $U_{dc}$-controlling station (red color).

## Scanning Frequency Range

From different publications, it is observed that the considered scanning frequency range is 1 to 1000 Hz. However, it may not be required to scan the frequency all the way up to 1000 Hz as the converter dynamics has an effect on the DC-side impedance in much lower frequency range. This is because the individual cells of an MMC have a quite high time constant even though the MMC converter has much lower time constant, i.e. a factor of $\frac{1}{100}$ lower. Furthermore, the bandwidths of outer control loops (which mostly impact on the DC-side impedance) are basically much lower than 1000 Hz. Besides, there could be a risk of low frequency instability (normally occurs at frequency below the bandwidths of outer control loops) which is caused by non-linearity in the control system [4] (due to voltage and current limitations).

Fig. 6 shows an example of the scanned DC-side impedances of $U_{dc}$-control and P-control stations for low frequencies. As it can be seen, there is a clear difference between $U_{dc}$-control and P-control modes in both $Z_{re}$ and $Z_{im}$ for frequencies below 1 Hz. On the other hand, the possible resonance frequency may be much lower than 1000 Hz in the case of a large line current limiting inductance on the DC-side (e.g. 100 mH). Thus, the possible range of scanning frequency depends on a number of factors, but in general, a range of 0.1 to 350 Hz may cover majority of applications.

### Impact of the AC Network on the Equivalent DC-side Impedance

The AC network strength could also impact on the scanned DC-side impedance. First, injecting a harmonic current ,as shown in Fig. 5, results in a cell voltage ripple (having the same frequency as the injected current) which in turn generates the corresponding side band AC voltages. Then, the generated AC voltages drive a distorted AC current through the equivalent impedances of the AC network and converter resulting in a distorted power flow into the converter. Finally, this distortion can be seen as an error in the control system which tries to compensate it. Therefore, the impact of the AC network strength on DC-side impedance could be more pronounced in some control modes. Fig. 7 shows an example of scanned DC-side impedances of MMC for both AC network short circuit ratios (SCRs) of 40 and 3 under the same control mode as well as same power level. As it can be observed, there is a clear impact of AC network SCR on both $Z_{re}$ and $Z_{im}$. Therefore, for stability analyzing, it may be necessary to scan the DC-side impedance for two extreme AC network conditions (i.e. very strong and very weak).

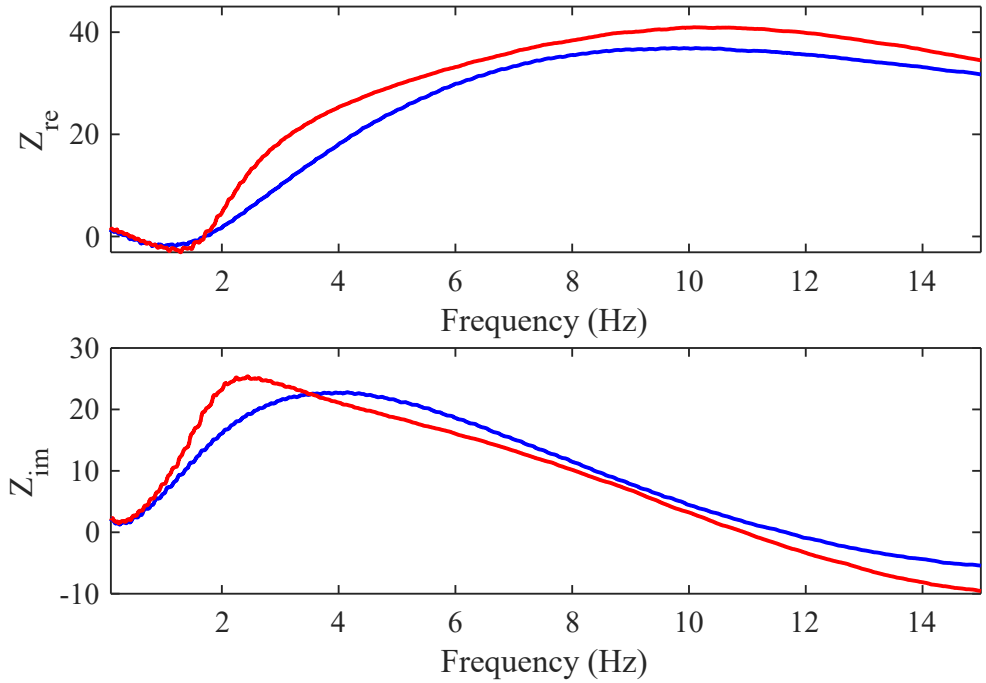


Fig. 7: Example of DC-side impedance of MMC showing the impact of AC network SCR while operating in $U_{dc}$-control mode. blue color: SCR=40 and red color: SCR=3.

### Impact of Load Level of Converter

In order to investigate the impact of the converter load, an example of scanned DC-side impedance of MMC for both inverter and rectifier modes of P-control station is shown in Fig. 8. As it can be seen, for inverter mode operation, the converter provides negative resistance as frequency approaches to zero; while for rectifier mode operation, it is opposite way. The similar test can be done for the $U_{dc}$-control station, and it is observed that there is no similar effect on the resistance when it changes from positive load to negative load. This is an expected behavior for P-controlling station and $U_{dc}$-controlling station.

### Impact of DC System Configuration

It is worth mentioning that although it may not be realistic to design rigid-bipolar in a DC grid, it should be possible to operate with partial rigid-bipolar in the case of damage to one section of metallic return

line. Thus, it is also worthwhile to investigate the impact of a change to the operating configuration on the DC-side impedance. It may be noted that the pole balancing is achieved via balancing current when the station is grounded (direct or indirect via metallic return), and the pole balancing is achieved via balancing voltage when the station is not grounded as in rigid-bipolar. Fig. 9 shows a comparison of the positive pole impedances from the ground return setup and the rigid-bipolar setup for both $U_{dc}$-control and P-control stations. From these results, it can be concluded that the configuration change has no impact on the DC-side impedance as far as the balancing control works as expected meaning steady-state balance is maintained.

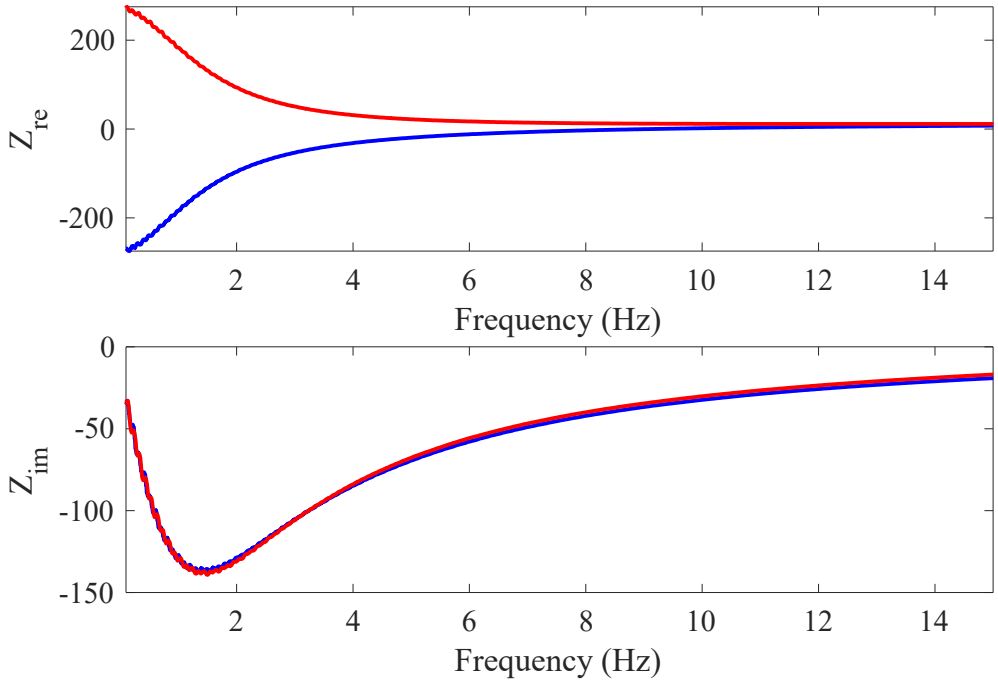


Fig. 8: Example of DC-side impedance of MMC showing the impact of load level of converter while operating in P-control mode. blue color: inverter mode and red color: rectifier mode.

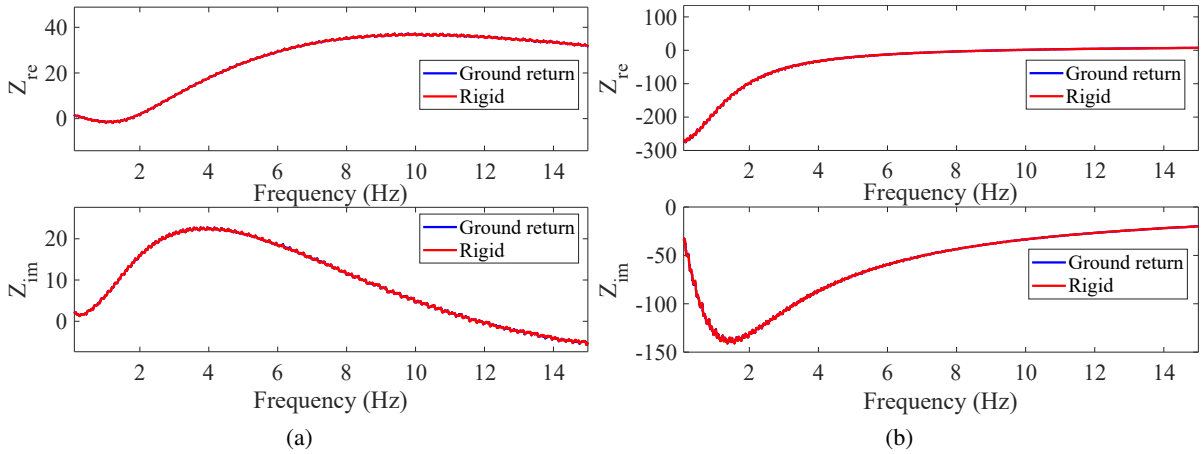


Fig. 9: Comparison of impedance of the positive pole converter seen from the DC-side in a bipolar with ground return (blue color) and rigid-bipolar (red color) configurations. (**a**) $U_{dc}$-control; (**b**) P-control.

## Conclusion

The DC-side impedance scanning as well as its corresponding circuit setups have been discussed in this paper. Some typical simulation results of the scanned DC side impedances have been presented. The

study experience and results have given the following conclusions and recommendations:

1. The DC-side impedance seen for the P-control station is different from the one for the DC control station justifying that impedance seen from the DC-side depends on various control modes.
2. The rectifier and inverter operations give significantly different resistance at very low frequency (close to zero frequency) in P-control mode. However, in $U_{dc}$-control mode, the impedance is not affected by the power flowing direction.
3. It is advisable to consider the AC network strength when scanning DC-side impedance, and it may be sufficient to consider two boundary conditions meaning the network conditions with minimum and maximum SCRs.
4. The DC-side impedance obtained in the monopole configuration is the same as the impedance when the same converter operates together with the other pole converter, i.e, balanced poles operation in the bipolar configuration. Thus, it may be adequate to perform the stability analysis in a monopole setup which could make the analysis significantly simplified.

## Appendix

The simulation throughout this paper has been implemented in PSCAD/EMTDC using the system parameters detailed in Table I.

Table I: System parameters

| Parameter | | Value |
|---|---|---|
| Point-to-point HVDC Link | $U_{ac,rated}$ | 400 kV |
| | $P_{rated}$ | 1000 MW (per pole) |
| | $U_{dc,rated}$ | 525 kV |
| | $f_0$ | 50 Hz |

## References


[1] PROMOTioN. Deliverable 12.4: Final Deployment Plan; Technical Report, PROMOTioN Project; PROMOTioN–Progress on Meshed HVDC Offshore Transmission Networks: Arnhem, The Netherlands, 2020.

[2] Rodriguez, Pedro, and Kumars Rouzbehi. "Multi-terminal DC grids: challenges and prospects." Journal of Modern Power Systems and Clean Energy 5.4 (2017): 515-523.

[3] Nghiem, A., and I. Pineda. "Wind Energy in Europe: Scenarios for 2030; WindEurope: Brussels, Belgium, 2017." https://windeurope.org/wp-content/uploads/files/about-wind/reports/Wind-energy-in-Europe-Scenarios-for-20 30: 32.

[4] prEN 50388-2:2017: "Railway Applications – Fixed installations and rolling stock – Technical criteria for the coordination between traction power supply and rolling stock to achieve interoperability – Part 2: stability and harmonics".

[5] BestPaths, "Deliverable D9.3: BEST PATHS DEMO#2 Final Recommendations for Interoperability of Multivendor HVDC Systems".

[6] Lyu, Jing, Xu Cai, and Marta Molinas. "Impedance modeling of modular multilevel converters." IECON 2015-41st Annual Conference of the IEEE Industrial Electronics Society. IEEE, 2015.

[7] Jamshidifar, Aliakbar, and Dragan Jovcic. "Small-signal dynamic DQ model of modular multilevel converter for system studies." IEEE Transactions on Power Delivery 31.1 (2015): 191-199.

[8] Li, Zhenyu, et al. "Accurate impedance modeling and control strategy for improving the stability of DC system in multiterminal MMC-based DC grid." IEEE Transactions on Power Electronics 35.10 (2020): 10026-10049.

[9] A. Antonopoulos, et al. "On Dynamics and Voltage Control of the Modular Multilevel Converter" 2009 13th European Conference on Power Electronics and Applications.

[10] Saad, Hani, Albane Schwob, and Yannick Vernay. "Study of resonance issues between HVDC link and power system components using EMT simulations." 2018 Power Systems Computation Conference (PSCC). IEEE, 2018.

[11] Sun, Jian. "Impedance-based stability criterion for grid-connected inverters." IEEE transactions on power electronics 26.11 (2011): 3075-3078.

[12] Quester, Matthias, et al. ”Online impedance measurement of a modular multilevel converter.” 2019 IEEE PES Innovative Smart Grid Technologies Europe (ISGT-Europe). IEEE, 2019.
[13] Quester, Matthias, et al. ”Frequency behavior of an MMC test bench system.” 2020 6th IEEE International Energy Conference (ENERGYCon). IEEE, 2020.
[14] Liao, Yicheng, et al. ”Stability and Sensitivity Analysis of Multi-Vendor, Multi-Terminal HVDC Systems.” arXiv preprint arXiv:2111.12013 (2021).
[15] F. Loku et al. “Equivalent Impedance Calculation Method for Control Stability Assessment in HVDC Grids,” MDPI Energies 2021, 14, 6899. Available at: https://www.mdpi.com/1996-1073/14/21/6899/pdf.
[16] Yang, Dongsheng, et al. ”Automation of impedance measurement for harmonic stability assessment of mmc-hvdc systems.” 18th Wind Integration Workshop. 2019.
[17] H. Wu et al. “Development of an AC/DC Impedance Matrix Measurement Toolbox for MTDC System,” 20th Wind Integration Workshop, November 2021.